

Effect of Pendulation on an $SO(3)$ -Based Attitude Estimator for Precision Pointing of an Atmospheric Balloon-Borne Platform

David Evan Zlotnik* and James Richard Forbes†

Department of Aerospace Engineering, University of Michigan, Ann Arbor, Michigan, 48109, USA

Attitude estimation of a balloon-borne platform is considered. Specifically, the effects of pendulation on an $SO(3)$ -based attitude estimator is investigated. The balloon platform is modelled as a rigid-body hanging from a three-dimensional pendulum representing a tether. The $SO(3)$ -based estimator is implemented and the acceleration due to oscillation is included in the accelerometer measurements. Four simulations are conducted that demonstrate the effects of oscillation on the estimator. It is shown that the estimation error due to oscillation can be mitigated by reducing the estimator gain associated with the accelerometer.

I. Introduction

Many balloon-borne robotic systems require an adequate attitude control system for proper operation. For example, a balloon-borne observatory must orient itself to a high degree of accuracy to properly observe celestial objects. Attitude control systems rely on an attitude estimate generated by sensors. The attitude of balloon-borne platforms, or any rigid-body, is uniquely and globally described by rotation matrices, the set of matrices belonging to the special orthogonal group denoted $SO(3)$. However, rotation matrices are rarely used directly within estimation algorithms. Typically, attitude estimation is accomplished by utilizing the extended Kalman filter to estimate a quaternion, a rotation matrix parameterization. This approach is taken in Refs. 1, 2, and 3 for attitude estimation of balloon-borne platforms. When coupled with low-cost measurement units however, the extended Kalman filter is difficult to apply robustly.⁴

Rather than using rotation matrix parametrizations within an extended Kalman filter to estimate attitude, Refs. 4, 5, 6, and 7 consider estimators that evolve directly on $SO(3)$. In particular, Ref. 4 considers an estimator that provides estimates of the attitude as well as the gyroscope bias from measurements taken from typical low-cost inertial measurement units. These units contain an accelerometer and magnetometer for measurements of the gravitational and magnetic field vectors, as well as a gyroscope that provides angular velocity measurements. Assuming the accelerometer gives an accurate measurement of the gravitational field vector, the proposed estimator can be used to determine the attitude of a balloon-borne platform. However, if the platform is subject to pendulation or oscillatory motion the accelerometer may not give accurate measurements of the gravitational field vector and the estimator could be adversely affected.

The purpose of this paper, and its main contribution, is to investigate the effects of pendulation on an $SO(3)$ -based nonlinear estimator for an atmospheric balloon-borne platform. To this end, the equations of motion of the platform are derived using a Lagrangian approach. The platform is considered as a rigid-body, and the tether connecting the platform to the balloon is modelled as a three dimensional pendulum. The estimator of Ref. 4 is implemented in simulation along with a simple proportional-derivative control law.

The remainder of this paper is as follows. Notation is discussed in Sec. II. In Sec. III the platform model is discussed and the kinematics and dynamics of the system are reviewed. The estimator is presented in Sec. IV and a proportional-derivative control law is implemented. The platform dynamics are simulated in Sec. V and closing remarks are given in Sec. VI.

*Ph.D. Precandidate. Address: FXB Building, 1320 Beal Avenue, Ann Arbor, Michigan, USA, 48109-2140. Telephone: +1 (734) 764 3310. Facsimile: +1 (734) 763 0578. Email: dzlotnik@umich.edu

†Assistant Professor. Address: FXB Building, 1320 Beal Avenue, Ann Arbor, Michigan, 48109-2140 USA. Telephone: +1 (734) 764 3310. Facsimile: +1 (734) 763 0578. Email: forbesrj@umich.edu

II. Preliminaries

A. Notation

This paper will adopt the notation found in Ref. 8. Briefly, a physical vector can be expressed as a linear combination of three unit physical vectors that form a basis for physical three-dimensional space. For example, the physical vector \underline{u} can be written as

$$\begin{aligned}\underline{u} &= \underline{a}_1 u_{a,1} + \underline{a}_2 u_{a,2} + \underline{a}_3 u_{a,3} \\ &= \begin{bmatrix} \underline{a}_1 & \underline{a}_2 & \underline{a}_3 \end{bmatrix}^T \begin{bmatrix} u_{a,1} \\ u_{a,2} \\ u_{a,3} \end{bmatrix} \\ &= \underline{\mathcal{F}}_a^T \mathbf{u}_a,\end{aligned}$$

where $\underline{\mathcal{F}}_a$ is the vectrix associated with reference frame “ a ”, denoted \mathcal{F}_a , and $\mathbf{u}_a \in \mathbb{R}^3$ is a column matrix containing the components of \underline{u} resolved in \mathcal{F}_a .^{8,9} The cross product of two physical vectors, $\underline{u} \times \underline{v}$, can be resolved in \mathcal{F}_a as

$$\begin{aligned}\underline{u} \times \underline{v} &= (\underline{\mathcal{F}}_a^T \mathbf{u}_a) \times (\underline{\mathcal{F}}_a^T \mathbf{v}_a) \\ &= \mathbf{u}_a^T \underline{\mathcal{F}}_a \times \underline{\mathcal{F}}_a \mathbf{v}_a \\ &= \underline{\mathcal{F}}_a^T \mathbf{u}_a^\times \mathbf{v}_a,\end{aligned}$$

where $(\cdot)^\times : \mathbb{R}^3 \rightarrow \mathfrak{so}(3)$ with $\mathfrak{so}(3) = \{\mathbf{S} \in \mathbb{R}^{3 \times 3} | \mathbf{S}^T = -\mathbf{S}\}$ such that⁸

$$\mathbf{u}_a^\times = \begin{bmatrix} 0 & -u_{a,3} & u_{a,2} \\ u_{a,3} & 0 & -u_{a,1} \\ -u_{a,2} & u_{a,1} & 0 \end{bmatrix}.$$

The orientation of one reference frame relative to another can be described by a direction cosine matrix. For example, consider the physical vector \underline{u} resolved in two reference frames, \mathcal{F}_b and \mathcal{F}_a , $\underline{u} = \underline{\mathcal{F}}_b^T \mathbf{u}_b = \underline{\mathcal{F}}_a^T \mathbf{u}_a$. The relationship between \mathbf{u}_a and \mathbf{u}_b can be found by taking the dot product of $\underline{\mathcal{F}}_b^T$ and \underline{u} ,

$$\begin{aligned}\underline{\mathcal{F}}_b^T \mathbf{u}_b &= \underline{\mathcal{F}}_a^T \mathbf{u}_a \\ \mathbf{u}_b &= \underline{\mathcal{F}}_b \cdot \underline{\mathcal{F}}_a^T \mathbf{u}_a \\ &= \mathbf{C}_{ba} \mathbf{u}_a,\end{aligned}\tag{1}$$

where $\mathbf{C}_{ba} = \underline{\mathcal{F}}_b \cdot \underline{\mathcal{F}}_a^T$ is the direction cosine matrix describing the orientation of \mathcal{F}_b relative to \mathcal{F}_a .⁸ Note that (1) can also be written as $\mathbf{u}_a = \mathbf{C}_{ba}^T \mathbf{u}_b = \mathbf{C}_{ab} \mathbf{u}_b$; \mathbf{C}_{ba}^T is often called a rotation matrix. The direction cosine matrix \mathbf{C}_{ba} also maps the components of a physical vector resolved in \mathcal{F}_a to \mathcal{F}_b . Direction cosine matrices belong to the special orthogonal group of rigid-body rotations denoted $SO(3)$, that is $SO(3) = \{\mathbf{C} \in \mathbb{R}^{3 \times 3} | \mathbf{C}^T \mathbf{C} = \mathbf{1}, \text{set}(\mathbf{C}) = +1\}$ where $\mathbf{1}$ is the identity matrix.

III. Platform Model

A dynamic model of a balloon-borne platform is considered in detail in Ref. 10. For completeness the kinematics and dynamics of this model will be reviewed here. Consider the platform model shown in Fig. 1. The platform itself is modelled as a rigid-body and is denoted \mathcal{R} . To model pendulation \mathcal{R} is constrained to move with a three dimensional pendulum, denoted \mathcal{P} . The pendulum is modelled as a rigid body. Body \mathcal{R} may rotate freely. A reference frame \mathcal{F}_b is attached to \mathcal{R} at its center of mass. Another Frame \mathcal{F}_p is attached to \mathcal{P} with its origin coinciding with the origin of an inertial frame, \mathcal{F}_a . The pendulum has one end pinned to the origin of \mathcal{F}_a and another pinned to \mathcal{R} at point o .

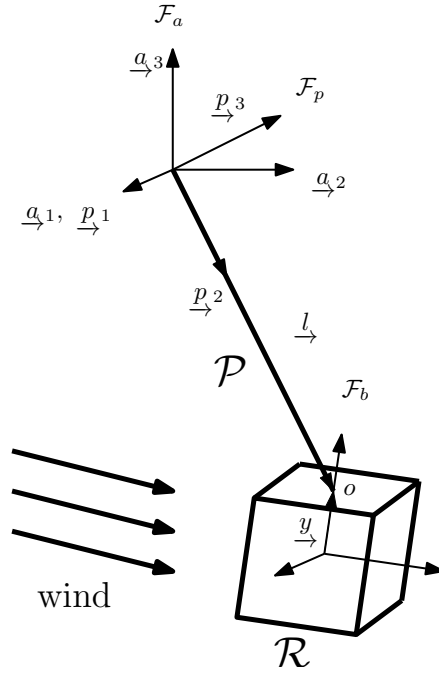


Figure 1. Platform model.

A. Kinematics

Let $\underline{\omega}^{ba} = \underline{\mathcal{F}}_b^T \underline{\omega}_b^{ba}$ and $\underline{\omega}^{pa} = \underline{\mathcal{F}}_p^T \underline{\omega}_p^{pa}$ be the angular velocities of \mathcal{F}_b and \mathcal{F}_p relative to \mathcal{F}_a , respectively. The orientations of \mathcal{F}_b and \mathcal{F}_p relative to \mathcal{F}_a are described by the direction cosine matrices \mathbf{C}_{ba} and \mathbf{C}_{pa} , respectively. The rotational kinematics of \mathcal{R} and \mathcal{P} are described by Poisson's equations,⁸

$$\dot{\mathbf{C}}_{ba} + \underline{\omega}_b^{ba \times} \mathbf{C}_{ba} = \mathbf{0},$$

and

$$\dot{\mathbf{C}}_{pa} + \underline{\omega}_p^{pa \times} \mathbf{C}_{pa} = \mathbf{0}.$$

In the analysis of the estimator that follows it will be necessary to consider the linear acceleration of \mathcal{R} . To this end, let \underline{r}^{ba} be the position of \mathcal{F}_b relative to \mathcal{F}_a . Referring to Fig. 1, $\underline{r}^{ba} = \underline{l} - \underline{y}$ where \underline{l} is the position of point o relative to \mathcal{F}_a and \underline{y} is the position of point o relative to \mathcal{F}_b . The velocity of \mathcal{F}_b relative to \mathcal{F}_a is

$$\begin{aligned} \underline{v}^{ba} = \underline{r}^{ba \cdot} &= \underline{l}^\circ + \underline{\omega}^{pa} \times \underline{l} - \underline{y}' - \underline{\omega}^{ba} \times \underline{y} \\ &= \underline{\omega}^{pa} \times \underline{l} - \underline{\omega}^{ba} \times \underline{y}, \end{aligned}$$

where $(\cdot)^\bullet$, $(\cdot)^\circ$, and $(\cdot)'$ are time derivatives with respect to \mathcal{F}_a , \mathcal{F}_p , and \mathcal{F}_b , respectively. The acceleration of \mathcal{F}_b relative to \mathcal{F}_a can be found to be

$$\begin{aligned} \underline{a}^{ba} = \underline{v}^{ba \cdot} &= \underline{\omega}^{pa \circ} \times \underline{l} + \underline{\omega}^{pa} \times \underline{\omega}^{pa} \times \underline{l} - \underline{\omega}^{ba'} \times \underline{y} - \underline{\omega}^{ba} \times \underline{\omega}^{ba} \times \underline{y} \\ &= \underline{\mathcal{F}}_b^T \left(\mathbf{C}_{bp} (\dot{\underline{\omega}}_p^{pa \times} \mathbf{I}_p + \underline{\omega}_p^{pa \times} \underline{\omega}_p^{pa \times} \mathbf{I}_p) - \dot{\underline{\omega}}_b^{ba \times} \mathbf{y}_b - \underline{\omega}_b^{ba \times} \underline{\omega}_b^{ba \times} \mathbf{y}_b \right) \\ &= \underline{\mathcal{F}}_b^T \mathbf{a}_b^{ba}, \end{aligned} \tag{2}$$

where $\mathbf{C}_{bp} = \mathbf{C}_{ba} \mathbf{C}_{pa}^T$, and \mathbf{a}_b^{ba} is the acceleration of \mathcal{F}_b relative \mathcal{F}_a resolved in \mathcal{F}_b .

B. Dynamics

Using Lagrange's equation for constrained systems the equations of motion of the platform model are

$$\mathbf{M}(\boldsymbol{\theta}^{ba}, \boldsymbol{\theta}^{pa})\dot{\boldsymbol{\nu}} + \boldsymbol{\tau}_{non}(\boldsymbol{\nu}) = \boldsymbol{\tau}^d + \boldsymbol{\tau}^c, \quad (3)$$

where $\mathbf{M}(\boldsymbol{\theta}^{ba}, \boldsymbol{\theta}^{pa})$ is the systems mass matrix, $\boldsymbol{\nu} = [\boldsymbol{\omega}_b^{ba\top} \ \boldsymbol{\omega}_p^{pa\top}]^\top$, $\boldsymbol{\tau}_{non}(\boldsymbol{\nu})$ is a vector of nonlinear effects, $\boldsymbol{\tau}^d$ is the disturbance torque, $\boldsymbol{\tau}^c$ is the control torque, and $\boldsymbol{\theta}^{ba}$ and $\boldsymbol{\theta}^{pa}$ are Euler angles associated with \mathbf{C}_{ba} and \mathbf{C}_{pa} , respectively. For more details on the derivation of the equations of motion, see Ref. 10.

IV. Estimation and Control

A. Estimation

The estimation algorithm, including gyroscope bias estimation, presented in Ref. 4 and Ref. 5 will now be used for attitude estimation of the balloon-borne platform. Assume that, along with an angular velocity measurement, two vector measurements are available. Specifically, the two measurements are the Earth's gravitational field vector from an accelerometer and Earth's magnetic field vector from a magnetometer. Let $\underline{\mathbf{g}}$ and $\underline{\mathbf{m}}$ be the physical vectors corresponding to the Earth's gravitational field and magnetic field, respectively. These vectors are measured in the body frame and the magnetometer measurement is modelled as

$$\mathbf{m}_b^y = \mathbf{C}_{ba}\mathbf{m}_a + \boldsymbol{\mu}^m,$$

where \mathbf{m}_b^y is the measured magnetic field vector resolved in the body frame, \mathbf{m}_a is the true magnetic field vector resolved in the inertial frame, and $\boldsymbol{\mu}^m$ is zero mean Gaussian noise associated with the magnetometer.

Ignoring the acceleration of \mathcal{F}_b relative to \mathcal{F}_a for the moment, the accelerometer measurement may be similarly modelled as

$$\mathbf{g}_b^y = \mathbf{C}_{ba}\mathbf{g}_a + \boldsymbol{\mu}^g, \quad (4)$$

where \mathbf{g}_b^y is the measured measured gravitational field vector resolved in the body frame, $\mathbf{g}_a = [0 \ 0 \ -g]^\top$ is the true gravitational field vector resolved in the inertial frame, $g = 9.81 \text{ (m/s}^2\text{)}$ is the acceleration due to gravity, and $\boldsymbol{\mu}^g$ is zero mean Gaussian noise associated with the accelerometer. Ordinarily, this accelerometer model is accurate as the acceleration due to gravity is much larger than $\|\mathbf{a}_b^{ba}\|_2$ at low frequencies.⁵ However, low frequency oscillations of the balloon-borne platform during flight can cause significant accelerometer disturbances. In order to investigate this effect this paper will consider the following accelerometer model:

$$\mathbf{g}_b^y = \mathbf{C}_{ba}\mathbf{g}_a + \mathbf{a}_b^{ba} + \boldsymbol{\mu}^g, \quad (5)$$

where the linear acceleration of \mathcal{F}_b relative to \mathcal{F}_a has been included in the accelerometer measurement.

Let \mathbf{C}_{ea} be the estimate of \mathbf{C}_{ba} . The direction cosine matrix \mathbf{C}_{ea} describes the orientation of an estimator frame relative to the inertial frame \mathcal{F}_a . Consider the estimator dynamics,^{4,5}

$$\dot{\mathbf{C}}_{ea} = -(\boldsymbol{\omega}^y + \boldsymbol{\sigma} - \hat{\mathbf{b}})^\times \mathbf{C}_{ea}, \quad (6)$$

and

$$\dot{\hat{\mathbf{b}}} = -\frac{k_i}{k} \boldsymbol{\sigma}, \quad (7)$$

where \mathbf{C}_{ea} is the rotation matrix estimate, $\boldsymbol{\omega}^y = \boldsymbol{\omega}_b^{ba} + \mathbf{b} + \boldsymbol{\mu}$ is the measured angular velocity, \mathbf{b} is the gyroscope bias, $\boldsymbol{\mu}$ is the gyroscope measurement noise, $\hat{\mathbf{b}}$ is the estimate of \mathbf{b} , $\boldsymbol{\sigma}$ is the innovation, and $0 < k_i < \infty$ and $0 < k < \infty$ are constant gains that must be tuned.⁴ The innovation must be chosen such that \mathbf{C}_{ea} approaches \mathbf{C}_{ba} asymptotically. For this purpose, the innovation $\boldsymbol{\sigma}$ has the form

$$\boldsymbol{\sigma} = -k(k_g \mathbf{g}_e^\times \mathbf{g}_b^y + k_m \mathbf{m}_e^\times \mathbf{m}_b^y), \quad (8)$$

where $0 < k_g < \infty$ and $0 < k_m < \infty$ are constant gains, $\mathbf{g}_e = \mathbf{C}_{ea}\mathbf{g}_a$ and $\mathbf{m}_e = \mathbf{C}_{ea}\mathbf{m}_a$ are the estimates of \mathbf{g}_a and \mathbf{m}_a expressed in the estimator frame, respectively.⁴ The constant gains k_g and k_m are typically chosen based on the relative confidence in the accelerometer and magnetometer measurements. For example, $k_g > k_m$ indicates a higher confidence in the accelerometer compared to the magnetometer measurements.

The filter described by Refs. 5, 6, and 7 must be discretized before it can be used on hardware. The discretized form of (6) is

$$\mathbf{C}_{ea}^{k+1} = \mathbf{A}^k \mathbf{C}_{ea}^k,$$

where $\mathbf{A}^k = \exp(\hat{\boldsymbol{\omega}}^{k \times})$ is given by^{4,11}

$$\mathbf{A}^k = \mathbf{1} - \hat{\boldsymbol{\omega}}^{k \times} \frac{\sin(|\hat{\boldsymbol{\omega}}^k|T)}{|\hat{\boldsymbol{\omega}}^k|} + \left(\hat{\boldsymbol{\omega}}^{k \times}\right)^2 \frac{1 - \cos(|\hat{\boldsymbol{\omega}}^k|T)}{|\hat{\boldsymbol{\omega}}^k|^2},$$

and $\hat{\boldsymbol{\omega}} = \boldsymbol{\omega}^y + \boldsymbol{\sigma} - \hat{\mathbf{b}}$. In addition, Eq. (7) is discretized as⁵

$$\hat{\mathbf{b}}^{k+1} = \hat{\mathbf{b}}^k - T \frac{k_i}{k} \boldsymbol{\sigma},$$

where T is the sample time.

B. Control

Consider a simple proportional-derivative controller:

$$\tau_c = -k_p \hat{\theta}_3 - k_d (\omega_3^y - \hat{b}_3),$$

where $\hat{\theta}_3$ is the estimated yaw angle of the platform extracted from \mathbf{C}_{ea} , ω_3^y is the third component of the measured angular velocity, \hat{b}_3 is the third component of the estimated bias, and $0 < k_p < \infty$ and $0 < k_d < \infty$ are the proportional and derivative control gains, respectively.

V. Simulation

The estimation and control algorithm presented in Secs. IV.A and IV.B will now be implemented in simulation. To compare the effect of oscillation on the estimator four simulations are conducted. The following parameters are common to all simulations. The initial angular velocity and initial attitude of the platform is $\boldsymbol{\omega}_b^{ba}(0) = [0 \ 0 \ 0.1]^T$ (rad/s) and $\mathbf{C}_{ba}(0) = \mathbf{C}_1(0^\circ)\mathbf{C}_2(0^\circ)\mathbf{C}_3(20^\circ)$, where \mathbf{C}_i , $i = 1, 2, 3$ are principal rotations about the 1, 2 and 3 axes. The desired attitude of the platform is $\mathbf{C}_{da} = \mathbf{C}_1(\theta_1)\mathbf{C}_2(\theta_2)\mathbf{C}_3(0^\circ)$ where θ_1 and θ_2 are arbitrary. The initial pendulum angular velocity and attitude is $\boldsymbol{\omega}_p(0) = [0 \ 0 \ 0]^T$ (rad/s) and $\mathbf{C}_{pa}(0) = \mathbf{C}_1(-85^\circ)\mathbf{C}_2(0^\circ)\mathbf{C}_3(0^\circ)$, respectively. The control gains are $k_p = 1.5$ ($N \cdot m$) and $k_d = 0.5$ ($N \cdot m \cdot s$). During simulation, the plant model is numerically integrated using a fourth-order Runge-Kutta integrator with a time-step of 0.005 (s). The initial attitude estimate is $\mathbf{C}_{ea}(0) = \mathbf{1}$. The gyroscope bias is $\mathbf{b} = 0.05[1 \ 1 \ 1]^T$ (rad/s) and the initial bias estimate is $\hat{\mathbf{b}}(0) = [0 \ 0 \ 0]^T$ (rad/s). The noise covariance matrices associated with the accelerometer, magnetometer, and gyroscope measurements are $\mathbf{R}^g = \text{diag}\{\sigma_g^2, \sigma_g^2, \sigma_g^2\}$, $\mathbf{R}^m = \text{diag}\{\sigma_m^2, \sigma_m^2, \sigma_m^2\}$, and $\mathbf{R}^\omega = \text{diag}\{\sigma_\omega^2, \sigma_\omega^2, \sigma_\omega^2\}$, where $\sigma_g = 0.005$ (m/s^2), $\sigma_\omega = 0.005$ (rad/s), and $\sigma_m = 0.01$ ($A \cdot m^2$). It is assumed that $\mathbf{m}_a = 1/\sqrt{3}[1 \ 1 \ 1]^T$ ($A \cdot m^2$). The estimator gain k is set to $k = 5$. In the simulation measurements become available every 0.04 (s). In addition, the platform is affected by a disturbance torque populated by data taken from an uncontrolled balloon flight.¹² For more information on this flight and the implementation of the disturbance see Refs. 10 and 12.

In the first two simulations $k_g = k_m = 1$, indicating that the accelerometer and magnetometer measurements are weighted equally thereby having the same effect on the estimator. In one simulation (4) is used as the accelerometer model while in the other (5) is used. To distinguish between the two models in the following plots (4) will be referred to as model 1 and (5) will be referred to as model 2. The purpose of these two simulations is to demonstrate the effect of pendulation on the estimator when the accelerometer and magnetometer measurements are assumed to be of the same confidence level. Figures 2 and 3 demonstrate the attitude estimate error. In Fig. 2 the trace of $\mathbf{C}_{be} = \mathbf{C}_{ba}\mathbf{C}_{ea}^T$ is plotted. Note that $\mathbf{C}_{be} = \mathbf{1}$ indicates that $\mathbf{C}_{ea} = \mathbf{C}_{ba}$ and the attitude estimate is identically equal to the true attitude. Thus, $\text{tr}(\mathbf{C}_{be}) = 3$ indicates that $\mathbf{C}_{ea} = \mathbf{C}_{ba}$. In Fig. 3 the yaw error, pitch error, and roll error extracted from \mathbf{C}_{be} are plotted. The norm of the bias error $\|\mathbf{b} - \hat{\mathbf{b}}\|_2$ is plotted in Fig. 4. These plots indicate that the introduction of the linear acceleration of the platform into the accelerometer measurements introduce significant estimation errors.

In the next two simulations, $k_g = 0.1$ and $k_m = 1$. This is an effort to mitigate the effects of accelerometer disturbances due to platform oscillations by reducing the relative confidence of acceleration measurements

in the estimator. Again, the attitude estimation error for both accelerometer models is presented in Figs. 5 and 6. The bias estimation error is plotted in Fig. 7. Although the estimator takes longer to converge, it is clear that by reducing the value of k_g the effects of oscillation on the estimator are mitigated. The estimator more closely resembles the case when accelerations due to oscillation are not included in the accelerometer measurements.

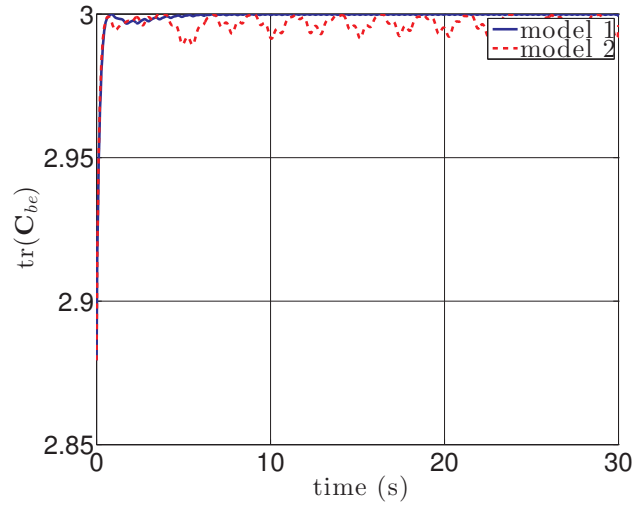


Figure 2. $k_g = k_m = 1$; $\text{tr}(\mathbf{C}_{be})$ versus time.

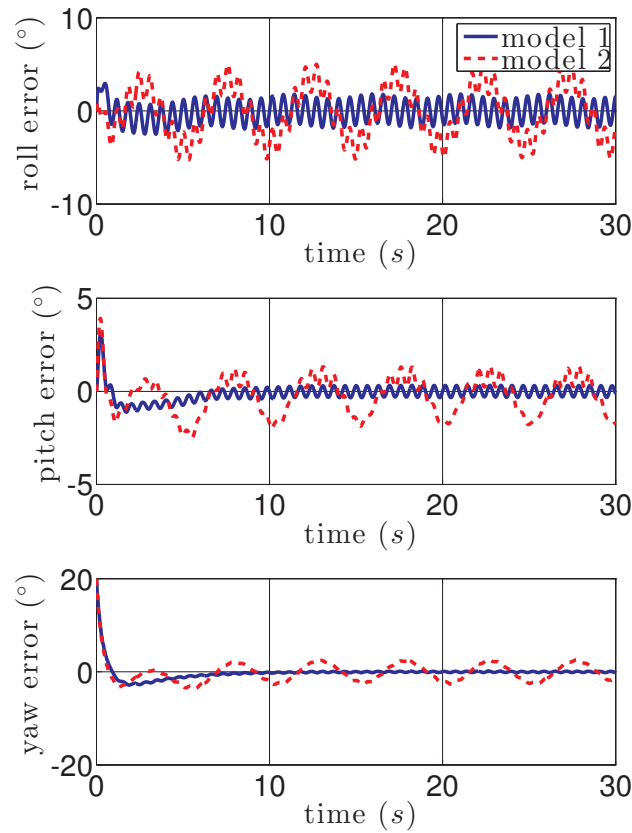


Figure 3. $k_g = k_m = 1$; yaw, pitch, and roll error versus time.

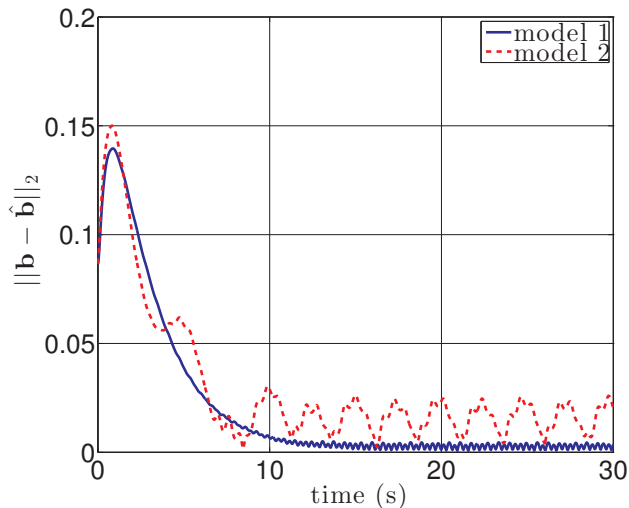


Figure 4. $k_g = k_m = 1$; bias estimate error versus time.

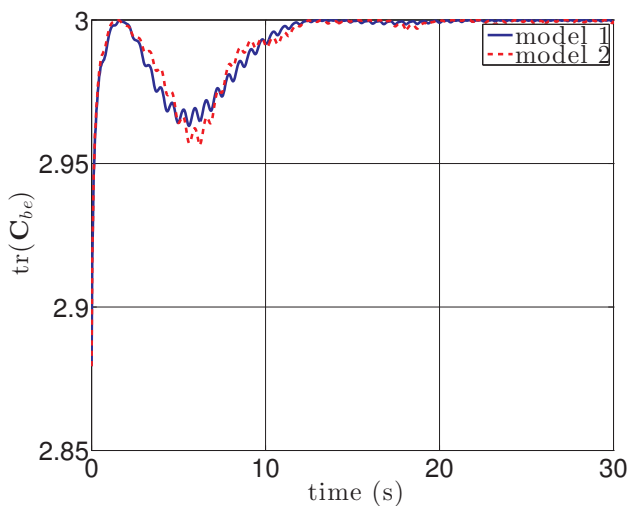


Figure 5. $k_g = 0.1, k_m = 1$; $\text{tr}(\mathbf{C}_{bee})$ versus time.

VI. Conclusions

In this paper the effects of platform oscillation on a nonlinear $SO(3)$ -based estimator has been investigated. Accelerometer, magnetometer, and gyroscope measurements are used to construct the estimator presented in Refs. 4 and 5. A proportional-derivative control law is used to control the yaw angle of the balloon-borne platform. The acceleration of the balloon-borne platform due to oscillation is included in the accelerometer measurement and the effects of this acceleration on the estimator was demonstrated in simulation. It was shown that the effects of oscillation can be mitigated by reducing the estimator gain associated with the accelerometer. Thus, when oscillations of a balloon-borne platform become significant it is advantageous to reduce the accelerometer gain. Future work includes the development of an estimator which incorporates acceleration due to oscillation directly within the estimator formulation.

VII. Acknowledgements

The authors would like to thank Nguyen Khoi Tran and the rest of the McGill High Altitude Ballooning team for the acquisition of flight data used in this paper.

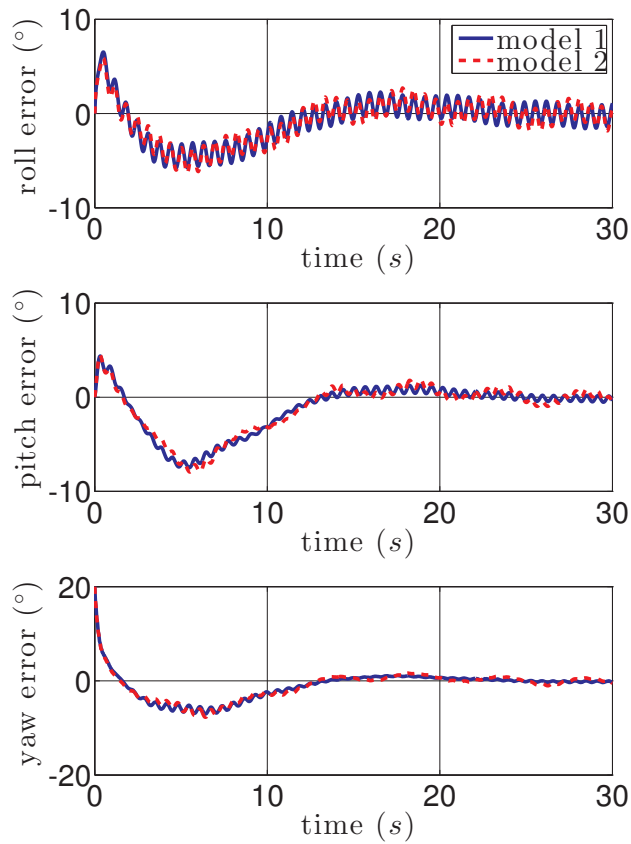


Figure 6. $k_g = 0.1$, $k_m = 1$; yaw, pitch, and roll error versus time.

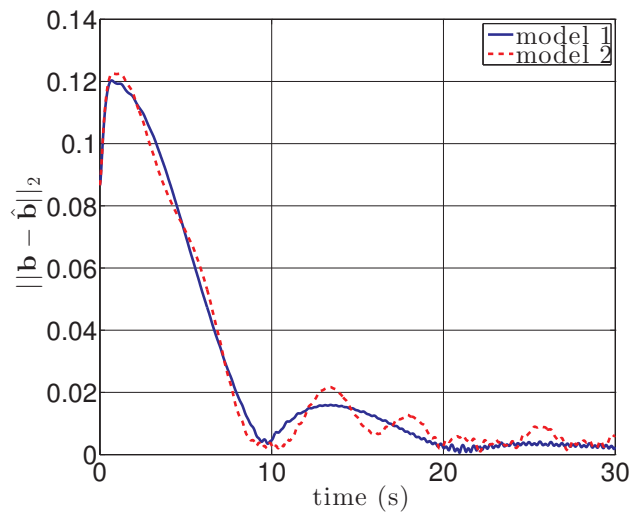


Figure 7. $k_g = 0.1$, $k_m = 1$; bias estimate error versus time.

References

¹Quine, B. M., Strong, K., Wiacek, A., Wunch, D., Anstey, J. A., and Drummond, J. R., “Scanning the Earth’s limb from a high-altitude balloon: The development and flight of a new balloon-based pointing system,” *Journal of Atmospheric and Oceanic Technology*, Vol. 19, No. 5, 2002, pp. 618–632.

²Pascale, E., Ade, P., Bock, J., Chapin, E., Chung, J., Devlin, M., Dicker, S., Griffin, M., Gundersen, J., Halpern, M.,

et al., “The balloon-borne large aperture submillimeter telescope: BLAST,” *The Astrophysical Journal*, Vol. 681, No. 1, 2008, pp. 400.

³Buccilli, T., Folina, A., Medaglia, E., Montefusco, P., Oliva, M., Palmerini, G., and Sestito, A., “A low cost inertial navigation experiment onboard balloons,” *Proc. 19th ESA Symposium on European Rocket and Balloon Programmes and Related Research, Bad Reichenhall, Germany*, June 2009.

⁴Mahony, R., Hamel, T., and Pfimlin, J.-M., “Complementary filter design on the special orthogonal group $SO(3)$,” *IEEE Conference on Decision and Control*, Dec. 2005, pp. 1477 – 1484.

⁵Hamel, T. and Mahony, R., “Attitude estimation on $SO(3)$ based on direct inertial measurements,” *IEEE International Conference on Robotics and Automation*, May 2006, pp. 2170 –2175.

⁶Mahony, R., Hamel, T., and Pfimlin, J.-M., “Nonlinear complementary filters on the special orthogonal group,” *Automatic Control, IEEE Transactions on*, Vol. 53, No. 5, 2008, pp. 1203–1218.

⁷Khosravian, A. and Namvar, M., “Globally exponential estimation of satellite attitude using a single vector measurement and gyro,” *IEEE Conference on Decision and Control*, Dec. 2010, pp. 364–369.

⁸Hughes, P. C., *Spacecraft Attitude Dynamics*, Dover, Mineola, New York, 2nd ed., 2004.

⁹de Ruiter, A., Damaren, C., and Forbes, J., *Spacecraft Dynamics and Control: An Introduction*, Wiley, 2013.

¹⁰Zlotnik, D. E. and Forbes, J. R., “Dynamic modeling, estimation, and control for precision pointing of an atmospheric balloon platform,” *Transactions of the Canadian Society for Mechanical Engineering*, Vol. 38, No. 2, 2014.

¹¹Murray, R., Li, Z., and Sastry, S., *A Mathematical Introduction to Robotic Manipulation*, CRC, 1994.

¹²Tran, N. K., He, X., Zlotnik, D. E., and Forbes, J. R., “Attitude sensing and control of a stratospheric balloon platform,” *AIAA Balloon Systems Conference, Daytona Beach, Florida, March 26-28, 2013*.